Research Article | Vol. 12, No. 7 / 1 Jul 2022 / Optical Materials Express 2426
Optical Materials EXPRESS

Rapid prototyping of silica optical fibers

PAWEL MANIEWSKI,* CLARISSA M. HARVEY, KORBINIAN MÜHLBERGER, TARAS ORIEKHOV, MARTIN BRUNZELL, FREDRIK LAURELL, AND MICHAEL FOKINE

Laser Physics Group, Department of Applied Physics, KTH Royal Institute of Technology, Stockholm, Sweden
pawelma@kth.se

Abstract: We demonstrate a method for rapid prototyping of optical fibers. Silica-based glass rods were 3D printed using laser powder deposition. Different doping of the 3D printed rods is evaluated, including alumina, titania, and erbium-doped glass. The rods were subsequently used as the core material in preforms with optical fibers drawn using a laser-based draw tower. A transmission loss of 3.2 dB/m was found for a fiber with 1 wt% titania doped core and pure silica cladding. Using this fabrication method, prototyping from powder to optical fiber could be achieved within a few hours.

1. Introduction

Optical fibers can be fabricated using various materials and compositions depending on the specific applications [1–4]. The fibers are typically drawn from performs, which are a scaled-up assembly of the desired fiber. To achieve low transmission losses, homogeneous, ultra-high purity materials are required. For silica-based compositions, this can be obtained using e.g., modified chemical vapor deposition (MCVD), which is commonly used for specialty fiber fabrication [5]. The prepared preform is subsequently heated above the softening point enabling a thin optical fiber to be drawn. The preform fabrication, together with the fiber drawing process is both time-consuming and costly, especially when studying a range of different compositions towards optimizing fiber properties.

Additive manufacturing (AM) techniques has shown great potential to shorten production cycles and reduce costs during low-volume production and prototyping. Recently, various glass AM techniques have been proven suitable for the manufacturing of polymer- and glass-based devices used in optics and photonics [6–9]. Today, silica glass AM can typically be achieved using two main approaches. In the first one, silica nanocomposite liquids, resins, or thermoplastics are used [10–12]. Here the object, referred to as the greenbody, is formed by 3D printing using, e.g., stereolithography or fused deposition modeling. The greenbody is then processed at elevated temperatures to remove the organic material. This is followed by high-temperature sintering, forming the final glass body. Fibers drawn from preforms using this approach have shown transmission losses on the order of 10 dB/m [13,14]. The second approach utilizes laser-based heating to melt or fuse either glass fibers [9,15,16], or sinter glass powders [17–22]. Laser sintering of powders, typically results in glass having a high degree of porosity [19–21]. However, it has been shown that by using sub-micron silica powders combined with mid-IR CO_2 laser melting the porosity of the printed glass can be significantly reduced, resulting in highly transparent objects [17,18,22].

In Laser Powder Deposition (LPD) a laser beam is used to locally melt the target and material is subsequently built by injecting powder into the laser-induced melt pool. In previous experiments, single component fumed silica powder with a purity of 99.8% was used [17,18]. However, tailoring the material properties through compositional variations can be achieved by sintering

#459400 https://doi.org/10.1364/OME.459400
Journal © 2022 Received 23 Mar 2022; revised 27 Apr 2022; accepted 28 Apr 2022; published 2 Jun 2022

Optical Materials EXPRESS

powder mixtures of different materials, as demonstrated for metals [23–25]. In glass, the main properties of interest are refractive index (RI) modification and doping with rare-earth (RE) ions to make laser active fibers. For optical fibers, GeO_2 is the standard dopant used to increase the RI of the light guiding core [1,26]. Other dopants that increase the RI include, e.g., titania (TiO_2) or alumina (Al_2O_3) [26–29]. Erbium doping is used in fiber amplifiers for optical telecommunication systems, while Ytterbium and Erbium-Ytterbium doping are commonly used for fiber lasers [1,5].

In this work, we demonstrate a procedure for rapid fabrication and prototyping, of optical fibers. Silica based glass rods doped with TiO_2, Al_2O_3, and Al_2O_3-Er_2O_3 were manufactured by LPD using a CO_2-laser. The rods were subsequently sleeved, using fused quartz tubes, to form the preform and then drawn into fibers. Changes in composition, and thereby core refractive index relative to the cladding tube, was achieved by mixing powdered dopants into fumed silica powder prior to LPD. Laser based systems, using a carbon monoxide (CO) laser, were used for preform assembly [30] and fiber drawing [31]. This, combined with the high deposition rate of LPD, a powder-to-fiber production could be achieved within a few hours, and potentially can be used to expedite the investigation of a wide range of core materials and specialty fiber compositions, where long lengths are not required.

2. Fiber fabrication

Three different laser-based setups were used for the fabrication of the optical fibers. These are schematically shown in Fig. 1. The LPD setup, shown in Fig. 1(a), was used to make doped silica rods used as the core material. A detailed description of the setup, which uses a CO_2-laser operating at 10.6 µm, can be found in Ref. [18]. Figure 1(b) shows the sketch of the system used for preform assembly and preparation. Here a glass lathe equipped with a CO-laser is used to process, collapse and taper the cladding tube and core rod. The preform system is described in detail in Ref. [30]. The prepared preforms were then mounted in a small draw tower and drawn into fiber. A CO-laser based furnace was used, schematically shown in Fig. 1(c), with details of the draw tower provided in Ref. [31].

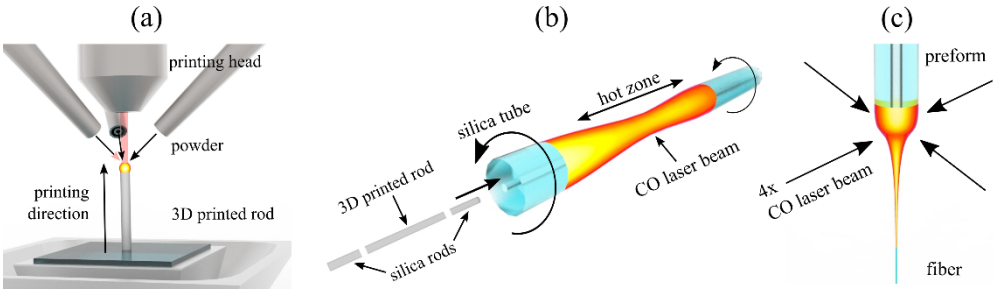

Fig. 1. Main fabrication steps: (a) 3D printing of the core material using a CO_2 laser; (b) sleeving the rod in a silica tube for preform assembly; (c) fiber drawing using a CO laser-based tower with four horizontal beams symmetrically heating the preform.

2.1. 3D printing of core rods

Silica based rods, used as core material, were 3D printed onto a fused quartz substrate (1 mm thick, PlanOptik AG). The substrate was locally melted by the incident CO_2 laser beam (ULR-50, Universal Laser Systems). The laser beam was focused onto the substrate using a single spherical lens (ZeSe, f = 40 mm) integrated within the print head. The print head also contained three powder feeding nozzles, which were placed around a centrally positioned laser beam, as shown in Fig. 1(a). Each nozzle was positioned approximately 9 mm away from the melt pool and the powder jets were aligned to intersect with the laser beam at the position of the melt pool [18].

Optical Materials EXPRESS

Table 1 shows the raw materials (powders) used in our experiments. The powders were carefully weighed (±0.01 g) and added to the silica powder in the ratios (labeled Ti-1, Ti-5, Ti-15, Al-2, Er-Al) specified in Table 2. The powders were then mixed using a stainless-steel ball mill until homogeneous, after which, 200 g of the mixture was loaded into the powder feeder in the LPD setup (Mark XV, Powder Dynamics Inc., modified for sub-micron powders [17]). For each print, a separate powder mixture was prepared.

Table 1. Powders used in the experiments.

Powder	Silica (SiO_2)	Titania (TiO_2)	Alumina (Al_2O_3)	Erbium Oxide (Er_2O_3)
Particle size [nm]	≈ 15	≤ 15	≤ 13	10-100
Purity [%]	99.8	99.5	99.8	99.9

Table 2. Powder mixtures used in the experiments.

	Ti-1	Ti-5	Ti-15	Al-2	Er-Al
Composition	TiO_2-SiO_2	TiO_2-SiO_2	TiO_2-SiO_2	Al_2O_3-SiO_2	Er_2O_3-Al_2O_3-SiO_2
Ratio [wt%]	1:99	5:95	15:85	2.5:97.5	0.3:3.4:96.3
Expected NA	0.09 Ref. [8,26]	0.121 Ref. [8,26]	-	-	0.14 Ref. [28]

During printing, powder was fed at a rate of 0.5 g/min, using technical air (Linde AB) as a carrier gas. Solid cylindrical rods were printed by vertical translation of the print head, while simultaneously feeding the powder. Deposition rates of doped silica glass of up to 1.3 mm^3/s were achieved, forming 20 mm long rods in approximately 20 seconds. The rods were then post-processed and pre-tapered to a diameter of approximately 1.1 mm as described in Ref. [18].

For each rod, a 2 mm long reference sample was cut off and polished on both ends to create a solid cylinder. These were used to measure the optical properties for the different glass compositions. The remaining sections of the rods were used as core material in fabrication of the optical fiber preforms.

2.2. Preform assembly

The prepared rods were placed into fused quartz tubes (Goodfellow) with outer and inner diameters of 6 mm and 1.1 mm, respectively. Two fused silica rods (1 mm diameter) were placed at opposite ends of the printed rod, sealing it at the center of the preform (see Fig. 1(b)). The rod-in-tube assembly was evacuated using approximately 15 mbar, collapsing the tube onto the printed rod while tapering to form a solid preform with a dimeter of 1.8 mm. This assembly was then re-sleeved and re-tapered to achieve the desired core to outer diameter (OD) ratio. The final preforms used in our experiments had an OD of 6 mm with a core diameter of approximately 250 µm. During processing, a laser power of up to 305 W, with a spot size of approximately 14.6 mm, was used to heat the rotating (100 RPM) rod-in-tube assembly to approximately 1800 °C (monitored with a pyrometer: Endurance Series, Fluke). A detailed description of the preform setup and preform fabrication process can be found in Ref. [30].

In order to investigate the properties of the 3D printed cores in isolation, the cladding was kept consistent by using this rod-in-tube assembly over fully 3D printed preforms.

2.3. Fiber drawing

The preforms were drawn into fibers, with an OD of 125 µm, using the CO laser-based draw tower described in Ref. [31]. The 2.8 m tall draw tower has all the standard components of a typical draw tower, except for the laser-based furnace. In this setup, the beam of the CO laser (Diamond

Optical Materials EXPRESS

J-3-5, Coherent) was split into four and redirected to intersect the preform symmetrically, as shown schematically in Fig. 1(c). The use of a compact laser-based furnace has several benefits, including a fast startup time, rapid temperature control, and an open architecture allowing in-situ monitoring of the neck-down region. Typical draws were performed at a draw speed of 20 m/min, with a tension up to approximately 0.3 N. Drawn fibers were coated using a high RI UV curable resin (OF-154 L, ShinEtsu).

In Fig. 2, photographs of the fabrication steps of the fiber Ti-15 are shown. Figure 2(a) shows LPD fabrication of the core rod, while Fig. 2(b) shows tapering during the final assembly of the preform. The highly doped Ti-15 core was clearly visible during processing and drawing, due to the higher emissivity of the core dopant compared to the silica cladding, as is clearly seen in Fig. 2(b) and 2(c). In Fig. 2(d), a micrograph of the resulting Ti-15 fiber, with the coating removed, is shown. Here, bottom illumination and a high contrast was used to further increase the visibility of the core.

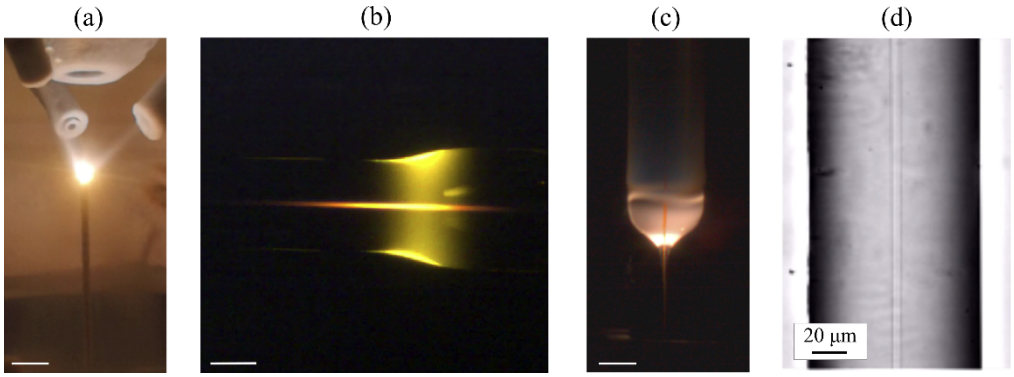

Fig. 2. Photographs of Ti-15 fiber fabrication: (a) LPD of core rod; (b) preform tube during collapse and tapering; (c) neckdown region of the preform during fiber drawing, (d) micrograph of the drawn fiber. White scale bars correspond to 3 mm.

2.4. Optical characterization

The optical transmission spectra of the reference samples of each 3D printed rod were measured, using a spectrophotometer (Cary50, Varian Inc).

The resulting fibers were cleaved and then examined using an optical microscope (Nikon Eclipse LV100). The fiber transmission was measured using the cut-back technique. A white light source (Whitelase SC480, Fianium) was coupled into a SMF-28 patch cable, which was then butt-coupled to the fiber under test. The transmitted light was measured in the range of 400 nm to 1800 nm using two power meters (S120C, 400 - 1100 nm, and S122C, 800 - 1800 nm, Thorlabs). Index-matching oil and fiber micro-bending were used during measurements to strip out cladding modes. This was confirmed by inspection of the near- and far-field pattern. The loss measurements were based on 7 to 12 consecutive cut-backs in steps of approximately 9 cm in length. The fiber loss was then calculated using an exponential fit.

To estimate the numerical aperture (NA), the output divergence angle for the different fibers were measured using a Gaussian fit to the mode diameter at known intervals. From the NA, the index step could also be estimated.

Optical Materials EXPRESS

3. Experimental results

3.1. Titania doped fibers

The micrographs of the resulting fibers: Ti-1, Ti-5, and Ti-15, are shown in Fig. 3(a), while the absorbance of the reference samples is shown in Fig. 3(b). The asymmetric shape of the fibers originated from uneven heating, due to slight furnace misalignment during the draw. The fiber cores, approximately 4 μm in diameter, were visible in all fibers. The fibers were found to cleave and splice easily using generic tools e.g., a diamond wheel cleaver, and a fusion splicer. Fiber Ti-1 showed an average loss of approximately 3.2 dB/m, with an NA of 0.020±0.001. Fiber Ti-5 had a loss of approximately 4.3 dB/m, with an NA of 0.024 ±0.001. The integrated losses were measured across the wavelength range of 400–1100 nm. Fiber Ti-15 was found to guide light and had an NA of 0.065 ±0.004, as shown in Fig. 3(c). However, losses were too high for reliable cut-back measurement.

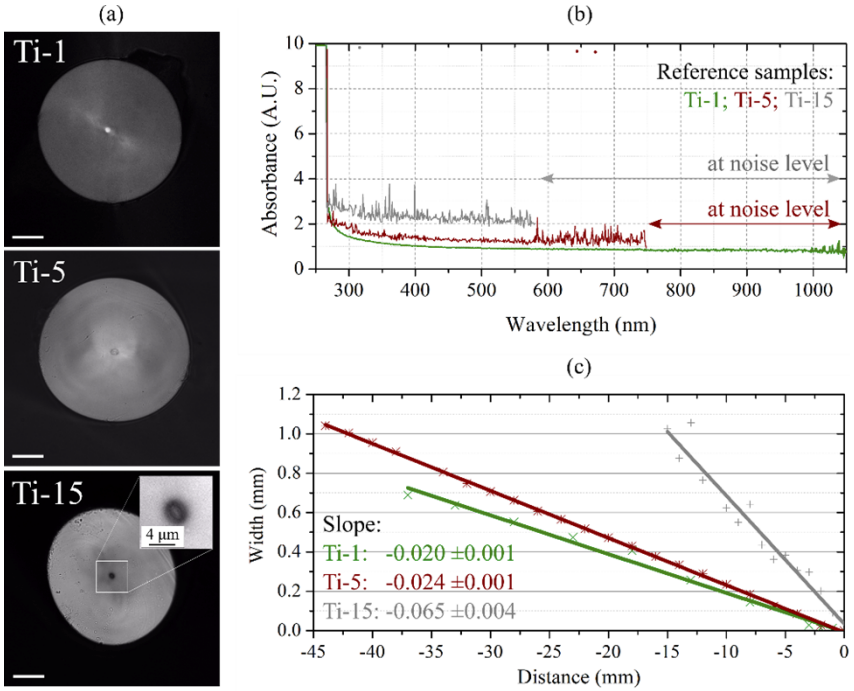

Fig. 3. The fibers (a) Ti-1, Ti-5, and Ti-15 (inset shows a magnification of the core). Scale bars correspond to 20 μm. (b) Absorbance of 2 mm long reference samples. (c) Width ($1/e^2$) of the output mode pattern (in far-field) from the resulting fibers. The solid lines correspond to linear fits with the slope and standard deviation of the fit given for each fiber.

3.2. Alumina doping

To evaluate Al_2O_3 doping, two 3D printed rods were studied; *(i)* rod doped with Al_2O_3 (powder Al-2, see Table 2) to evaluate a potential color-center formation during printing, and (*ii*) Er_2O_3-Al_2O_3 co-doped rod (powder Er-Al) to evaluate possible stimulated emission. Figure 4 shows the absorbance of the Al-2 reference sample. The absorbance of commercially available undoped fused silica and sample Ti-1, are included for comparison. The absorbance spectra of the fused silica and sample Al-2 were significantly lower in comparison to the Ti-doped rods. The spectra do not show any pronounced peaks.

Optical Materials EXPRESS

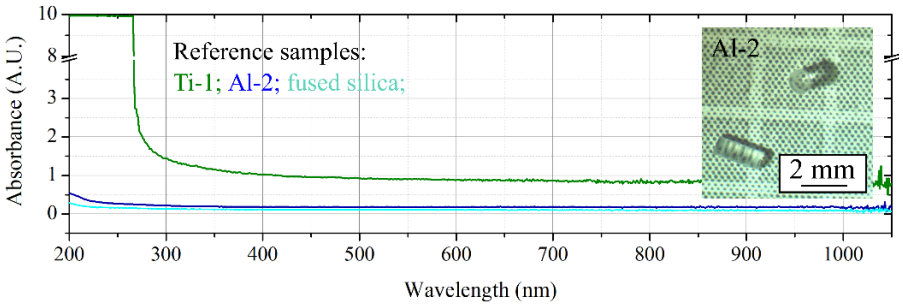

Fig. 4. The absorbance of Al-2 reference sample in comparison to commercial undoped fused silica rod, and 3D printed rod Ti-1. The inset shows Al-2 reference samples (side and top view).

3.3. *Er-Al doped active fiber*

In commercially available active fibers, alumina is typically used to increase the solubility of RE ions in silica [5]. Alumina doping can also be used to increase the RI in silica, enabling wave-guiding in silica fibers [27]. For the experiments performed here, the Er-Al powder mixture contained a slightly higher alumina content, compared to Al-2. This increased the step-index profile of the resulting fiber while also increasing the solubility of the RE ions in silica (see Table 2). Printing of the Er-Al doped rod was performed with a deposition rate of up to 1.1 mm^3/s, resulting in a diameter of approximately 1.3 mm. The rod is shown in Fig. 5(a). The

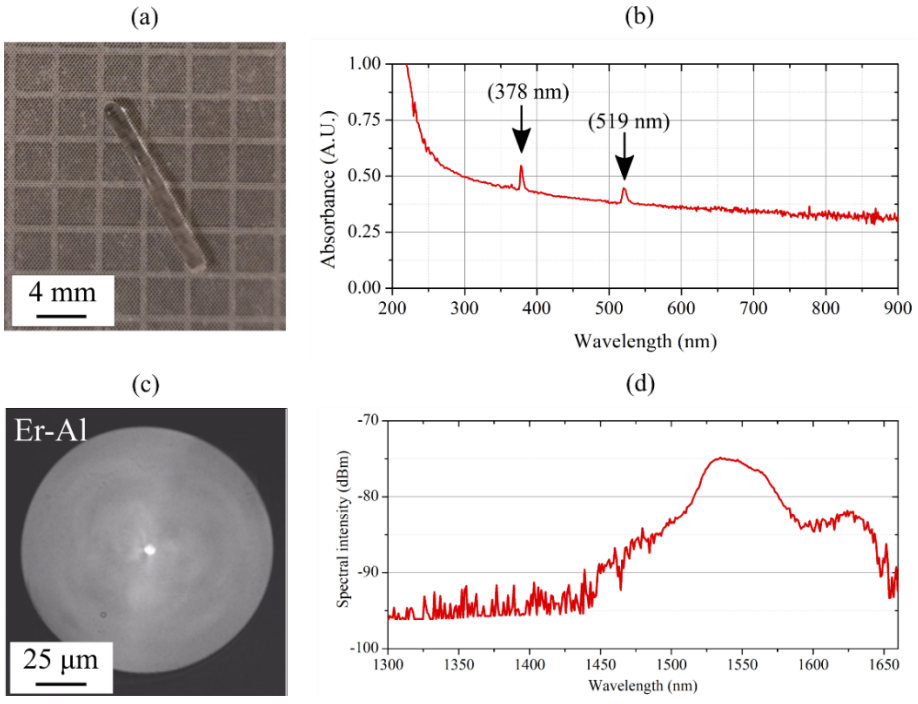

Fig. 5. Photograph (a) of 3D printed Er-Al rod, and (b) absorbance of the reference sample. (c) Bottom-lit micrograph of the Er-Al doped fiber. (d) Measured ASE spectra through ≈10 cm of fiber.

Optical Materials EXPRESS

absorbance spectrum of the Er-Al reference sample, shown in Fig. 5(b), contains two distinctive peaks at 519 nm and 378 nm, characteristic of Er^{3+} [5]. The Er-Al fiber was found to have a loss of approximately 13 dB/m, measured at $\lambda = 980$ nm, and approximately 4.5 dB/m, measured at $\lambda = 1550$ nm, with an NA of approximately 0.056 ±0.001.

To measure the emission spectrum, the fiber was pumped using a 976 nm laser diode (Thorlabs BL976-SAG300) with 60 mW of power. The output spectrum was monitored with an OSA (8614A, Hewlett Packard). The fiber was cut back until the maximum intensity of the ASE peak was observed, shown in Fig. 5. This occurred for a fiber length between 5 cm and 10 cm.

4. Discussion

A range of customized fibers with different glass composition were fabricated using the 3D printed rods. The rods contained different ratios of titania, alumina, and silica and were sleeved in quartz glass tubes, and successfully drawn into fibers. The absorbance spectra of the reference samples were comparable to the absorbance measured for previously reported samples doped with these elements [5,26,32].

The maximum length of the printed core rod was defined by the stroke range of the setup, which was 40 mm. Also, in these experiments, the diameter of the laser induced hot zone was 1.2 mm, which was slightly larger than the diameter of the three powder jets incident on the melt pool. However, the diameter of the resultant rod can easily be changed by adjusting the laser spot size. In future work, higher deposition rates can be achieved by increasing laser power, spot size, and powder feeding rate.

For fibers demonstrated here, in-coupling was performed manually in order to compensate for core offset due to asymmetry of the fibers. Further improvements of the draw procedure would improve roundness and core position, which would enable more reliable fusion splicing.

The lowest transmission loss of approximately 3.2 dB/m was measured for fiber Ti-1, which was printed using a silica powder mixture containing 1 wt% titania. With increasing titania concentration, measured losses in the Ti-doped fibers were found to increase. This was evident in the highly doped reference samples, Ti-5, and Ti-15, where a high absorbance was measured for wavelengths above 700 nm (see Fig. 3(b)). This can be expected as an increase in titania concentration leads to an increase in highly absorptive Ti^{3+}-related color-centers [1,26,32]. The formation of these color-centers can be attributed to the reduction of Ti^{4+}, which can take place at high processing temperatures when printing, processing the preform, and fiber drawing [1]. The titanium concentration within the core of these fibers corresponded to the initial powder mixture used for printing. This was verified by energy dispersive spectroscopy (EDS) measurements.

In the initial stage of this work, we used titania, as it was a commonly available sub-µm powder, which could be used to increase of RI of the printed glass. Despite the formation of color centers when using titania [1,26,32], the low-cost of the dopant was advantageous when empirically investigating deposition dynamics, as well as for optimizing mixing, feeding, and printing parameters.

In the first fiber produced (Ti-1) intermittent, elongated voids were found at the core-cladding interface. The length of these voids was typically shorter than a few hundred microns (< 400 µm) and less than half a micron in diameter, as shown in Fig. 6. They were spaced relatively evenly with several meters of void-free fiber in between. The formation of these voids was attributed to diameter variations along the printed Ti-1 core rod (1.10 mm ±0.05 mm). This prevented the cladding tube from fully collapsing during preform assembly, causing air-pockets to be trapped in the preform at the core-cladding interface. By adjusting printing parameters to reduce diameter variations, void-free fibers were subsequently produced. In future work, such voids can also be mitigated e.g., by progressing to a fully 3D printed preform where the cladding is directly printed onto the core in an additional LPD step.

Optical Materials EXPRESS

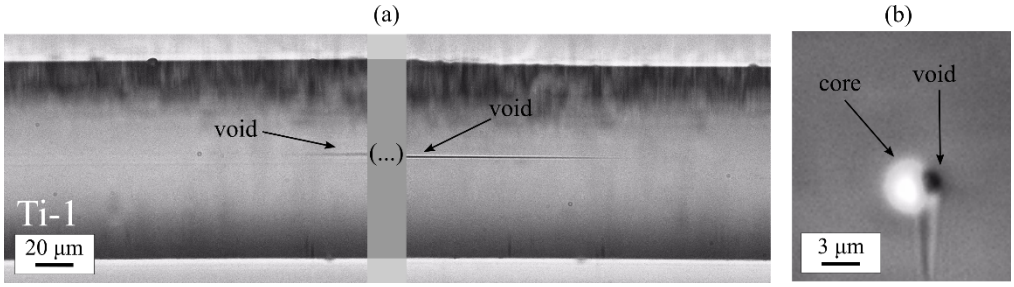

Fig. 6. Micrographs (a) of a core-cladding interface void found in fiber Ti-1, and (b) the corresponding cross-section.

By using alumina doped silica, transmission losses can be reduced as alumina typically forms fewer color centers compared to titania [27,28]. The Al-2 reference sample showed no apparent color-centers with an absorption spectrum comparable to commercial fused silica.

The Er-Al fiber had a measured NA of 0.056 ±0.001, which was lower than the value of 0.14 predicted using the initial dopant concentration in the powder mixture [28]. This discrepancy can be ascribed to a different deposition efficiency or evaporation rate of alumina during the LPD process. Investigation of the deposition efficiency for different dopants during LPD was outside the scope of this work and will require further study. However, the doping efficiency achieved in the resulting fiber was sufficient to generate ASE, successfully demonstrating this proof of concept. As such, the fiber may be used to construct a fiber laser operating at 1550 nm, which is currently under development.

5. Conclusions

In this work, 3D printed rods were used in the rapid prototyping of optical fibers. By using sub-micron powders and a CO_2 laser for Laser Powder Deposition, free-standing silica rods with different dopant concentrations were printed with a deposition rate of up to 1.3 mm^3/s. These cylindrical rods were subsequently used as the core material for the fabrication of optical fibers having different dopant compositions. Several hundreds of meters of each fiber were drawn using our in-house laser-based draw tower, although a standard draw tower would suffice. With the described procedure, including the use of our laser-based draw tower, full fiber fabrication could be completed in within a few hours. Produced fibers showed lower losses (3.2 dB/m) in comparison to fibers produced using other additive manufacturing techniques [13,14]. Furthermore, the Er_2O_3-Al_2O_3 co-doped active fiber demonstrated here, showed a characteristic amplified spontaneous emission peak at 1550 nm. In addition, using LPD, Ti-doped fibers were manufactured with dopant concentration as high as 15 wt% of titania.

The technique described in this work shows great potential for rapid prototyping of optical fibers, expediting the investigation of a wide range of core materials and fiber compositions.

Funding. Knut och Alice Wallenbergs Stiftelse (2016.0104); Stiftelsen för Strategisk Forskning (GMT14-0071, RMA150135).

Acknowledgments. We thank the Swedish Foundation for Strategic Research and the K.A. Wallenberg foundation for financial support.

Disclosures. The authors declare no conflicts of interest.

Data availability. Data underlying the results presented in this paper are not publicly available at this time but may be obtained from the authors upon reasonable request.

Optical Materials EXPRESS

References

1. J. Hecht, *City of Light: The Story of Fiber Optics* (Oxford, 1999).
2. A. Inoue and Y. Koike, "Low-noise graded-index plastic optical fiber for significantly stable and robust data transmission," J. Lightwave Technol. **36**(24), 5887–5892 (2018).
3. P. Kaiser and H. W. Astle, "Low-loss single-material fibers made from pure fused silica," Bell Syst. Tech. J. **53**(6), 1021–1039 (1974).
4. A. Schulzgen, L. Li, X. Zhu, V. L. Temyanko, and N. Peyghambarian, "Microstructured active phosphate glass fibers for fiber lasers," J. Lightwave Technol. **27**(11), 1734–1740 (2009).
5. M. Yamane and Y. Asahara, *Glasses for Photonics* (Cambridge University, 2000).
6. B. Assefa, M. Pekkarinen, H. Partanen, J. Biskop, J. Turunen, and J. Saarinen, "Imaging-quality 3D-printed centimeter-scale lens," Opt. Express **27**(9), 12630–12637 (2019).
7. E. N. Udofia and W. Zhou, "3D printed optics with a soft and stretchable optical material," Addit. Manuf **31**, 100912 (2020).
8. R. Dylla-Spears, T. D. Yee, K. Sasan, D. T. Nguyen, N. A. Dudukovic, J. M. Ortega, M. A. Johnson, O. D. Herrera, F. J. Ryerson, and L. L. Wong, "3D printed gradient index glass optics," Sci. Adv. **6**(47), eabc7429 (2020).
9. K. Rettschlag, A. Hohnholz, P. Jäschke, D. Kracht, S. Kaierle, and R. Lachmayer, "Laser glass deposition of spheres for printing micro lenses," Proc. CIRP **94**, 276–280 (2020).
10. F. Kotz, K. Arnold, W. Bauer, D. Schild, N. Keller, K. Sachsenheimer, T.M. Nargang, C. Richter, D. Helmer, and B.E. Rapp, "Three-dimensional printing of transparent fused silica glass," Nature **544**(7650), 337–339 (2017).
11. M. Mader, L. Hambitzer, P. Schlautmann, S. Jenne, C. Greiner, F. Hirth, D. Helmer, F. Kotz-Helmer, and B.B.E. Rapp, "Melt-extrusion-based additive manufacturing of transparent fused silica glass," Adv. Sci. **8**(23), 2103180 (2021).
12. D.G. Moore, L. Barbera, K. Masania, and A.R. Studart, "Three-dimensional printing of multicomponent glasses using phase-separating resins," Nat. Mater. **19**(2), 212–217 (2020).
13. Y. Chu, X. Fu, Y. Luo, J. Canning, Y. Tian, K. Cook, J. Zhang, and G.D. Peng, "Silica optical fiber drawn from 3D printed preforms," Opt. Lett. **44**(21), 5358–5361 (2019).
14. L. Angeles, C. Rosales, M. Núñez-Velázquez, and J.K. Sahu, "3D printed Er-doped silica fiber by Direct Ink Writing," *EPJ Web Conf.* 243 20002 (2020).
15. T. Grabe, M. Lammers, S. Wang, X. Wang, K. Rettschlag, K. Sleiman, A. Barroi, T. Biermann, A. Ziebehl, J. Röttger, P.-P. Ley, A. Wolf, P. Jaeschke, J. Hermsdorf, S. Kaierle, H. Ahlers, and R. Lachmayer, "Additive manufacturing of fused silica using coaxial laser glass deposition: experiment, simulation, and discussion," Proc. SPIE **11677**, 116770Z (2021).
16. J. Luo, J.M. Hostetler, L. Gilbert, J.T. Goldstein, A. M. Urbas, D. A. Bristow, R. G. Landers, and E.C. Kinzel, "Additive manufacturing of transparent fused quartz," Opt. Eng. **57**(4), 041408 (2018).
17. P. Maniewski, F. Laurell, and M. Fokine, "Laser cladding of transparent fused silica glass using sub-micron powder," Opt. Mater. Express **11**(9), 3056–3070 (2021).
18. P. Maniewski, F. Laurell, and M. Fokine, "Quill-free additive manufacturing of fused silica glass," Opt. Mater. Express **12**(4), 1480 (2022).
19. J. Luo, H. Pan, and E.C. Kinzel, "Additive manufacturing of glass," J. M. Sci. and Eng. **6**(136), 061024 (2014).
20. G. Marchelli, D. Storti, M. Ganter, and M. Prabhakar, "An introduction to 3D glass printing," *Solid Freeform Fabrication Symposium Proceedings, Austin, TX*, Aug. 3–5, 95–107 (2010).
21. M. Fateria, A. Gebhardta, S. Thuemmlera, and L. Thurna, "Experimental investigation on selective laser melting of glass," Phys. Procedia **56**, 357–364 (2014).
22. P. Maniewski, F. Laurell, and M. Fokine, "Reduction of shadowing effect during laser cladding of fused silica glass using sub-micron powders," Proc. SPIE **11677**, 1167711 (2021).
23. X. Zhang, S. Pfeiffer, P. Rutkowski, M. Makowska, D. Kata, J. Yang, and T. Graule, "Laser cladding of manganese oxide doped aluminum oxide granules on titanium alloy for biomedical applications," Appl. Surf. Sci. **520**, 146304 (2020).
24. W. Yuan, R. Li, Z. Chen, J. Gu, and Y. Tian, "A comparative study on microstructure and properties of traditional laser cladding and high-speed laser cladding of Ni45 alloy coatings," Surf. Coat. Technol. **405**, 126582 (2021).
25. E. Toyserkani, A. Khajepour, and S. F. Corbin, *Laser Cladding* (CRC, 2005).
26. C. L. Hoaglin and C. M. Truesdale, "Optical waveguide fiber containing titania and germania," US Patent, 5,841,933, (Nov. 24, 1998).
27. J. Wang, "Alumina as a dopant in optical fiber by OVD," Appl. Phys. A **116**(2), 505–518 (2014).
28. K.A.M. Sharif, N.Y.M. Omar, M.I. Zulkifli, S.Z.M. Yassin, and H.A. Abdul-Rashid, "Fabrication of alumina-doped optical fiber preforms by an mcvd-metal chelate doping method," Appl. Sci. **10**(20), 7231 (2020).
29. P.C. Schultz, "Binary titania-silica glasses containing 10 to 20 Wt% TiO_2," J. Am. Ceram. Soc. **59**(5-6), 214–219 (1976).
30. T. Oriekhov, C.M. Harvey, K. Mühlberger, and M. Fokine, "Specialty optical fiber fabrication: preform manufacturing based on asymmetrical CO laser heating," J. Opt. Soc. Am. B **38**(12), F130–F137 (2021).
31. C. M. Harvey, K. Mühlberger, T. Oriekhov, P. Maniewski, and M. Fokine, "Specialty optical fiber fabrication: fiber draw tower based on a CO laser furnace," J. Opt. Soc. Am. B **38**(12), F122–F129 (2021).

Optical Materials EXPRESS

32. P. Harshavardhan Reddy, M.F.A. Rahman, M.C. Paul, A.A. Latiff, A.H.A. Rosol, S. Das, A. Dhar, S. K. Bhadra, K. Dimyati, and S.W. Harun, "Titanium dioxide doped fiber as a new saturable absorber for generating mode-locked erbium doped fiber laser," Optik **158**, 1327–1333 (2018).